# Shapiro delay measurement of a 2 solar mass neutron star

P. Demorest[1], T. Pennucci[2], S. Ransom[1], M. Roberts[3] & J. W. T. Hessels[4,5]

October 29, 2010

1. National Radio Astronomy Observatory, 520 Edgemont Road, Charlottesville, VA 22093 USA

2. Astronomy Department, University of Virginia, Charlottesville, VA 22094-4325 USA

3. Eureka Scientific, Inc., Oakland, CA 94602, USA

4. Netherlands Institute for Radio Astronomy (ASTRON), Postbus 2, 7990 AA Dwingeloo, The Netherlands

5. Astronomical Institute "Anton Pannekoek," University of Amsterdam, 1098 SJ Amsterdam, The Netherlands

**Neutron stars are composed of the densest form of matter known to exist in our universe, and thus provide a unique laboratory for exploring the properties of cold matter at supranuclear density. Measurements of the masses or radii of these objects can strongly constrain the neutron-star matter equation of state, and consequently the interior composition of neutron stars[1, 2]. Neutron stars that are visible as millisecond radio pulsars are especially useful in this respect, as timing observations of the radio pulses provide an extremely precise probe of both the pulsar's motion and the surrounding space-time metric. In particular, for a pulsar in a binary system, detection of the general relativistic Shapiro delay allows us to infer the masses of both the neutron star and its binary**

**companion to high precision[3, 4]. Here we present radio timing observations of the binary millisecond pulsar PSR J1614−2230, which show a strong Shapiro delay signature. The implied pulsar mass of 1.97±0.04 M$_\odot$ is by far the highest yet measured with such certainty, and effectively rules out the presence of hyperons, bosons, or free quarks at densities comparable to the nuclear saturation density.**

In the accepted "lighthouse model" description of radio pulsars, a rapidly spinning neutron star (NS) with a strong magnetic field ($10^8$-$10^{15}$ G) emits a beam of radiation that is typically misaligned with the spin axis. A broadband, polarized pulse of radio emission is observed once per rotation if this beam crosses the Earth-pulsar line of sight. The extraordinary rotational stability of pulsars permits the precise measurement of a number of systematic effects that alter the arrival times of the radio pulses at Earth, a procedure referred to as pulsar timing. In the case of binary millisecond pulsars, which are the most stable pulsars with orbital companions, even typically subtle effects such as the general relativistic Shapiro delay can be revealed by timing. The Shapiro delay is an increase in light travel time through the curved space-time near a massive body. In binary pulsar systems that have highly inclined (nearly edge-on) orbits, excess delay in the pulse arrival times can be observed when the pulsar is situated nearly behind the companion during orbital conjunction. As described by general relativity, the two physical parameters that characterize the Shapiro delay are the companion mass and inclination angle. In combination with the observed Keplerian mass function, the Shapiro delay offers one of the most precise methods to directly infer the mass of the NS. In turn, any precise NS mass measurement limits the equations of state (EOS) available to describe matter at supranuclear densities. The discovery of a NS with mass significantly higher than the typical value of $\sim 1.4$ M$_\odot$ would have a major impact on the allowed NS EOS as well as additional implications for a wide range of astrophysical phenomena[5].

PSR J1614−2230 was originally discovered in a radio survey of unidentified EGRET gamma-ray sources using the Parkes radio telescope[6]. The spin period $P$ is 3.15 ms, and initial timing with Parkes showed the pulsar to be in a binary system with an 8.7-day orbital period and a companion of mass $M_2 \gtrsim 0.4$ M$_\odot$. The system was noted as having a higher companion mass than is typical for fully-recycled ($P \lesssim 10$ ms) pulsars, which predominantly have helium white dwarf (WD) companions with masses of $\sim 0.1 - 0.2$ M$_\odot$. Furthermore, the orbital period is shorter than expected given the massive

2

companion[7]. These facts hinted at a possible non-standard evolutionary history for the binary system (see below).

Following the inital discovery observations, J1614−2230 was observed regularly as a test source for several observing projects at the NRAO Green Bank Telescope (GBT)[8][†]. These data provide a continuous long-term timing record from mid-2002 to the present, and they show a marginally significant Shapiro delay signal. However, the data quality and arbitrary scheduling with respect to the binary's orbital phase made it impossible to obtain meaningful mass and inclination measurements from those data alone. In March 2010, we performed a dense set of observations of J1614−2230, timed to follow the system through one complete orbit with special attention paid to the orbital conjunction, where the Shapiro delay signal is strongest. These data were taken with the newly built Green Bank Ultimate Pulsar Processing Instrument[9]. GUPPI coherently removes interstellar dispersive smearing from the pulsar signal, and integrates the data modulo the current apparent pulse period, producing a set of average pulse profiles, or flux-versus-rotational-phase lightcurves. We observed an 800 MHz wide band centered at a radio frequency of 1.5 GHz. The raw profiles were then polarization- and flux-calibrated and averaged into 100-MHz, 7.5-minute intervals using the PSRCHIVE software package[10]. From these, pulse times of arrival were determined using standard procedures, with a typical uncertainty of ∼1 $\mu$s.

The measured arrival times are used to determine key physical parameters about the neutron star and its binary system by fitting them to a comprehensive timing model which accounts for every rotation of the neutron star over the time spanned by the fit. The model predicts at what times pulses should arrive at Earth, taking into account pulsar rotation and spin-down, astrometric terms (sky position, proper motion), binary orbital parameters, interstellar dispersion, and general relativistic effects such as the Shapiro delay (see Table 1). The observed arrival times are compared with the model prediction, and best-fit parameters are obtained via $\chi^2$ minimization, using the TEMPO2 software package[11][‡]. The post-fit residuals, i.e. the difference between the observed and model-predicted pulse arrival times, effectively measure how well the timing model describes the data, and are shown in Figure 1. We included both the older long-term datasets and our new

[†]The National Radio Astronomy Observatory is a facility of the U.S. National Science Foundation (NSF), operated under cooperative agreement by Associated Universities, Inc.
[‡]We also obtained consistent results using the original TEMPO package.

GUPPI data in a single fit. The long-term data determine model parameters with characteristic timescales longer than a few weeks (e.g. spin-down rate and astrometry), while the new data best constrain parameters on timescales of the orbital period or less. Both are necessary to reduce covariance between particular model parameters.

In addition to the physical timing model parameters listed in Table 1, the fit included arbitrary time offsets ("jumps") between different observing systems, and allowance for a time-variable interstellar dispersion measure (DM), a quantity proportional to the total free electron column density along the line of sight. A single DM value was fit for the long-term data set. The newer, more precise GUPPI data required a separate DM be fit for each day. DM is expected to vary on 1-day and longer timescales due to the relative motions of the pulsar and Earth through the interstellar medium[12]. We also investigated the possibility of DM variation on minute to hour timescales which could indicate the presence of excess gas in the binary system itself. If present, especially near orbital conjunction, this effect could bias the Shapiro delay measurement. However, we found no evidence of this in our data – we limit any such orbital DM variation to a level of $\lesssim 2 \times 10^{-4}\,\mathrm{pc\,cm^{-3}}$, corresponding to delays of $\lesssim 0.4\,\mu\mathrm{s}$ at a frequency of $1.5\,\mathrm{GHz}$. Furthermore, we observed orbital conjunctions at three different epochs over a span of 2 months, and all show consistent timing results without needing to model fast DM variation.

As shown in Figure 1, the Shapiro delay was detected in our data with extremely high significance, and must be included to correctly model the arrival times of the radio pulses. However, estimating parameter values and uncertainties can be tricky due to the high covariance between many orbital timing model terms, especially the Shapiro-derived companion mass ($M_2$) and inclination angle ($i$)[13]. In order to obtain robust error estimates, we used a Markov chain Monte Carlo (MCMC) approach to explore the post-fit $\chi^2$ space and derive posterior probability distributions for the model parameters (see Figure 2). In contrast with the common method of mapping $\chi^2$ projections in a reduced-dimensional parameter space[14, 3], MCMC is able to efficiently explore all fit dimensions simultaneously. Our final results for all timing model parameters, with MCMC error estimates, are given in Table 1. Due to the high significance of the detection, our MCMC procedure and the standard $\chi^2$ fit produce similar uncertainties.

From the detected Shapiro delay we measure a companion mass of $0.500\pm 0.006\,\mathrm{M_\odot}$, which implies that the companion is a helium-carbon-oxygen white

dwarf, as helium WD stars have masses of $\lesssim 0.45\,\mathrm{M_\odot}$[15]. Considering the 8.7-day orbital period, a likely formation mechanism for systems similar to J1614−2230 has been proposed[16, 17] where the original companion star is $\sim 3\,\mathrm{M_\odot}$. J1614−2230 is peculiar, however, in being fully recycled unlike the mildly-recycled pulsars ($P \sim 10 - 30\,\mathrm{ms}$) found in similar binary systems.

The Shapiro delay also shows the binary system to be amazingly edge-on, with an inclination of $89.17° \pm 0.02°$. This is the most inclined pulsar binary system currently known. The amplitude and sharpness of the Shapiro delay increase rapidly with increasing binary inclination and the overall scaling of the signal is linearly proportional to the mass of the companion star. Thus the unique combination of the high orbital inclination and massive WD companion in J1614−2230 cause a Shapiro delay amplitude orders of magnitude larger than for most other millisecond pulsars with $0.1 - 0.2\,\mathrm{M_\odot}$ companions and inclinations $\lesssim 75°$. In addition, the excellent timing precision achievable from the pulsar with the GBT and GUPPI provide a very high signal-to-noise ratio measurement of both Shapiro delay parameters within a single orbit.

The standard Keplerian orbital parameters, combined with known companion mass and orbital inclination, fully describe the dynamics of a "clean" binary system[§] under general relativity and therefore also determine the pulsar's mass. We measure a NS mass of $1.97 \pm 0.04\,\mathrm{M_\odot}$, by far the highest precisely measured NS mass determined to date. In constrast with X-ray based NS mass/radius measurements[18], the Shapiro delay provides no information about the NS radius. However, unlike the X-ray methods, our result is nearly model-independent, as it depends only on general relativity being an adequate description of gravity. In addition, unlike statistical pulsar mass determinations based on measurement of the advance of periastron[19, 20, 21], pure Shapiro delay mass measurements involve no assumptions about classical contributions to periastron advance or the distribution of orbital inclinations.

The mass measurement alone of a $1.97\,\mathrm{M_\odot}$ NS significantly constrains the NS EOS, as shown in Figure 3. Any proposed EOS whose mass-radius track does not intersect the J1614−2230 mass line is ruled out by this measurement. The EOSs which produce the lowest maximum masses tend to be those which predict significant softening past a certain central density. This is a common feature of models that include the appearance of "exotic" hadronic matter such as hyperons or kaon condensates at densities of a few times the nuclear

---

[§]A system comprised of two stable compact objects.

saturation density ($n_s$), for example GS1 and GM3 in Figure 3. All such EOSs are ruled out by our results. Our mass measurement does not completely rule out condensed quark matter as a component of the NS interior[22], but it does constrain quark matter model parameters, and excludes some strange quark matter models[5]. For the range of allowed EOS lines presented in Figure 3, typical values for the physical parameters of J1614−2230 are a central baryon density between $2-5\,n_s$ and a radius between $11-15\,$km, only $2-3$ times the Schwarzschild radius for a $1.97\,\mathrm{M_\odot}$ star. Based on EOS-independent analytic solutions of Einstein's equations, our mass measurement also sets an upper limit on the maximum possible mass density of cold matter[23], of $\lesssim 4 \times 10^{15}$ g cm$^{-3}$ $\sim$10 $n_s$.

The proposed formation mechanism for J1614−2230-like systems[16, 17] predicts that the neutron star would only accrete a few hundredths of a solar mass of material, much less than the $\sim$0.6 M$_\odot$ needed to bring a neutron star born at $1.4\,\mathrm{M_\odot}$ up to the observed pulsar mass. This implies either that the transfer of large amounts of mass onto the neutron star from the secondary is possible or alternatively that some neutron stars are born massive ($\sim$1.9 M$_\odot$). As the Shapiro delay has not been detected in most millisecond pulsar systems, our mass measurement for J1614−2230 suggests that many of these other systems may also harbor NSs with masses well above $1.4\,\mathrm{M_\odot}$.
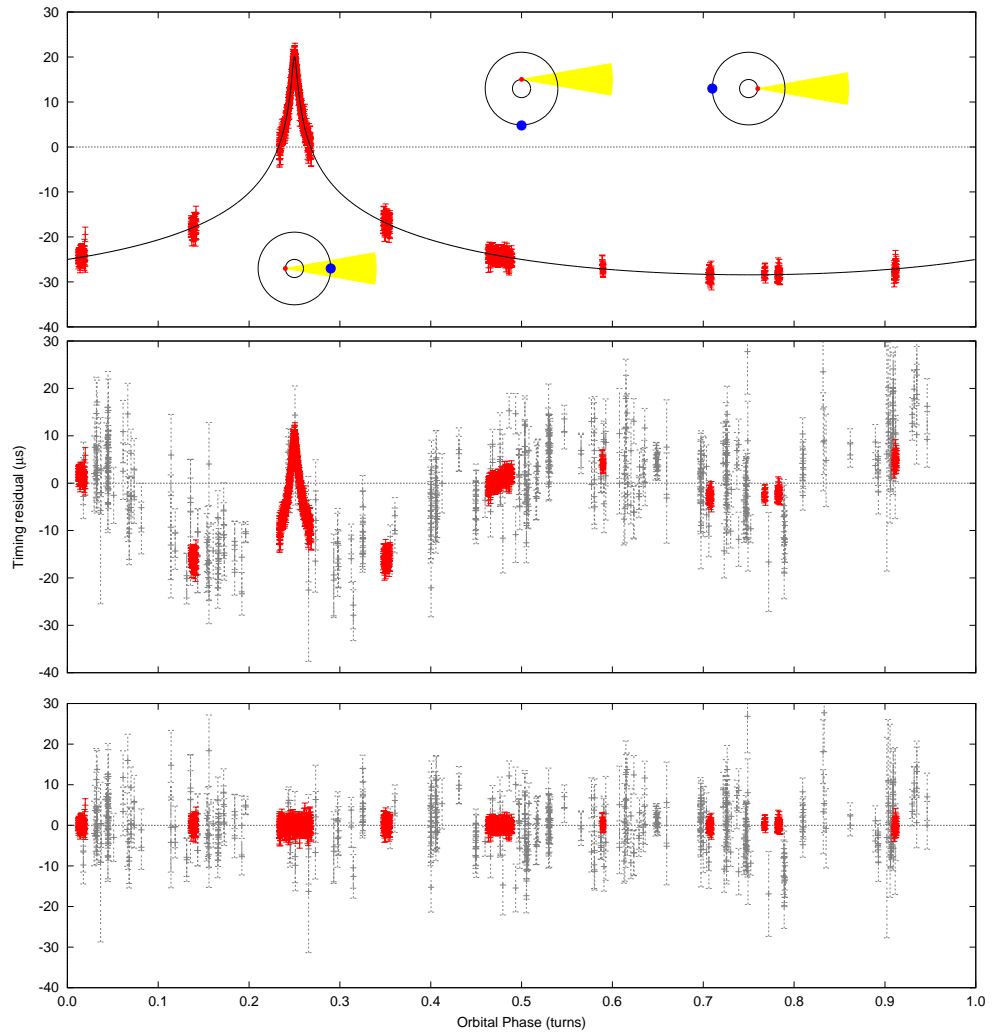
Figure 1: Shapiro delay measurement for PSR J1614−2230. Each panel shows timing residual – excess delay not accounted for by the timing model – as a function of the pulsar's orbital phase. The top panel shows the full magnitude of the Shapiro delay if it is not included in the timing model but with all other model parameters fixed at their best-fit values. The solid line shows the Shapiro delay functional form, and the red points are timing measurements from our GBT/GUPPI data set. The diagrams inset in this panel show a top-down schematic view of the binary system at orbital phases 0.25, 0.5, and 0.75. The neutron star is shown in red, the white dwarf companion in blue, and the emitted radio beam (yellow) points towards the Earth. At orbital phase 0.25, the Earth–pulsar line of sight passes nearest to the companion (∼240,000 km), producing the sharp peak in pulse delay. We found no evidence for any kind of pulse intensity variations, as from an eclipse, near conjunction. The middle panel shows the best-fit residuals obtained using an orbital model that does not account for general-relativistic effects. That the residuals deviate significantly from a random, Gaussian distribution of zero mean shows that the Shapiro delay must be included to properly model the pulse arrival times, especially at conjunction. In addition to the red GBT/GUPPI points, the gray points show the previous "long-term" data set described in the text. The dramatic improvement in data quality is apparent. Finally, the bottom panel shows the post-fit residuals for the fully relativistic timing model (including Shapiro delay), which have a root-mean-square residual of 1.1 $\mu$s and reduced $\chi^2$ value of 1.4 with 2165 degrees of freedom.

# References

[1] Lattimer, J. M. & Prakash, M. The Physics of Neutron Stars. *Science* **304**, 536–542 (2004).

[2] Lattimer, J. M. & Prakash, M. Neutron star observations: Prognosis for equation of state constraints. Phys. Rep. **442**, 109–165 (2007).

[3] Jacoby, B. A., Hotan, A., Bailes, M., Ord, S. & Kulkarni, S. R. The Mass of a Millisecond Pulsar. ApJ **629**, L113–L116 (2005).

[4] Verbiest, J. P. W. *et al.* Precision Timing of PSR J0437-4715: An Accurate Pulsar Distance, a High Pulsar Mass, and a Limit on the Variation
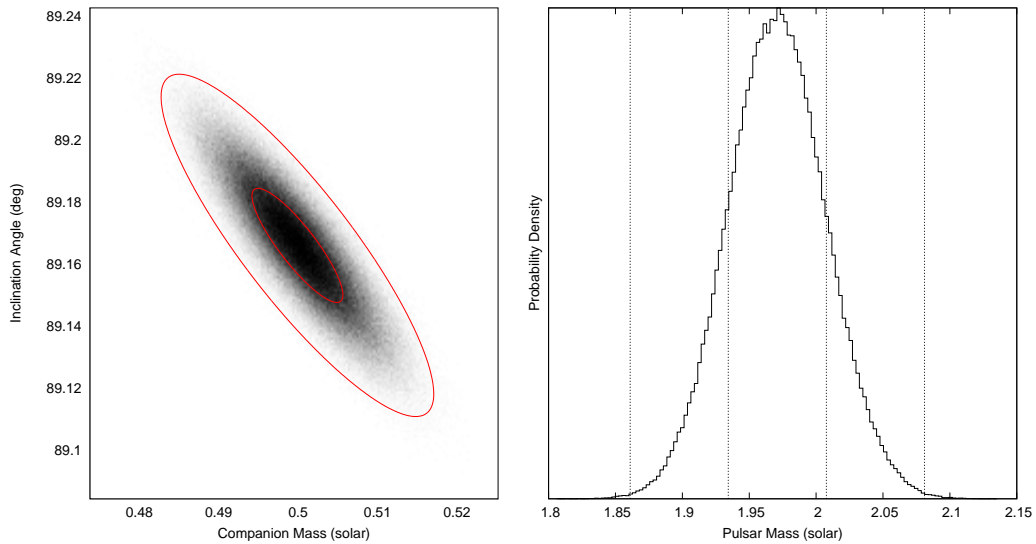
Figure 2: Results of the Markov chain Monte Carlo (MCMC) error analysis. The left panel grayscale shows the 2-D posterior probability density function (PDF) in the $M_2$-$i$ (companion mass versus orbital inclination) plane computed from a histogram of MCMC trial values. The ellipses show 1- and 3-$\sigma$ contours based on a Gaussian approximation to the MCMC results. The right panel shows the PDF for pulsar mass derived from the MCMC trials. In both cases the results are very well described by normal distributions due to the extremely high signal-to-noise ratio of our Shapiro delay detection.
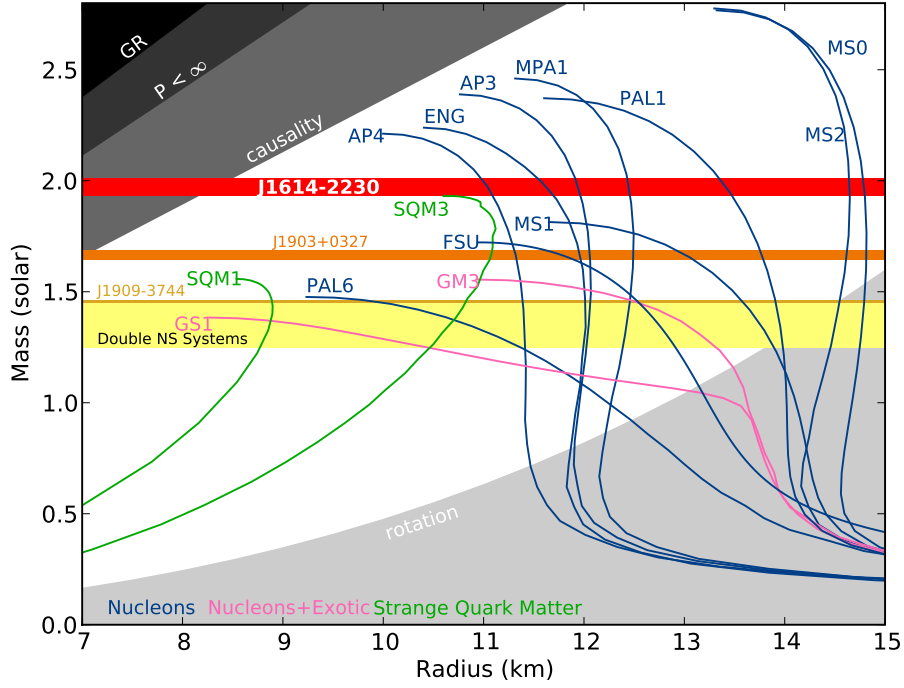
Figure 3: Neutron star (NS) mass-radius diagram. The plot shows non-rotating mass versus physical radius for several typical NS equations of state (EOS)[25]. The horizontal bands show the observational constraint from our J1614−2230 mass measurement of 1.97±0.04 $M_\odot$, similar measurements for two other millsecond pulsars[3, 26], and the range of observed masses for double NS binaries[2]. Any EOS line that does not intersect the J1614−2230 band is ruled out by this measurement. In particular, most EOS curves involving exotic matter, such as kaon condensates or hyperons, tend to predict maximum NS masses well below 2.0 $M_\odot$, and are therefore ruled out.

of Newton's Gravitational Constant. ApJ **679**, 675–680 (2008).

[5] Özel, F., Psaltis, D., Ransom, S. & Demorest, P. The Massive Pulsar PSR J16142230: Linking Quantum Chromodynamics, Gamma-ray Bursts, and Gravitational Wave Astronomy. *in prep* (2010).

[6] Hessels, J. *et al.* Three New Binary Pulsars Discovered With Parkes. In F. A. Rasio & I. H. Stairs (ed.) *Binary Radio Pulsars*, vol. 328 of *Astronomical Society of the Pacific Conference Series*, 395 (2005).

[7] Rappaport, S., Podsiadlowski, P., Joss, P. C., Di Stefano, R. & Han, Z. The relation between white dwarf mass and orbital period in wide binary radio pulsars. MNRAS **273**, 731–741 (1995).

[8] Ransom, S. *et al. in prep* (2010).

[9] Demorest, P. *et al.* GUPPI: The Green Bank Ultimate Pulsar Processing Instrument. *in prep* (2010).

[10] Hotan, A. W., van Straten, W. & Manchester, R. N. PSRCHIVE and PSRFITS: An Open Approach to Radio Pulsar Data Storage and Analysis. *Publications of the Astronomical Society of Australia* **21**, 302–309 (2004).

[11] Hobbs, G. B., Edwards, R. T. & Manchester, R. N. TEMPO2, a new pulsar-timing package - I. An overview. MNRAS **369**, 655–672 (2006).

[12] Ramachandran, R., Demorest, P., Backer, D. C., Cognard, I. & Lommen, A. Interstellar Plasma Weather Effects in Long-Term Multifrequency Timing of Pulsar B1937+21. ApJ **645**, 303–313 (2006).

[13] Damour, T. & Deruelle, N. General relativistic celestial mechanics of binary systems. II. The post-Newtonian timing formula. *Ann. Inst. Henri Poincaré Phys. Théor.* **44**, 263–292 (1986).

[14] van Straten, W. *et al.* A test of general relativity from the three-dimensional orbital geometry of a binary pulsar. Nature **412**, 158–160 (2001).

[15] Kippenhahn, R. & Weigert, A. *Stellar Structure and Evolution* (1990).

[16] Podsiadlowski, P. & Rappaport, S. Cygnus X-2: The Descendant of an Intermediate-Mass X-Ray Binary. ApJ **529**, 946–951 (2000).

[17] Podsiadlowski, P., Rappaport, S. & Pfahl, E. D. Evolutionary Sequences for Low- and Intermediate-Mass X-Ray Binaries. ApJ **565**, 1107–1133 (2002).

[18] Özel, F. Soft equations of state for neutron-star matter ruled out by EXO 0748 - 676. Nature **441**, 1115–1117 (2006).

[19] Ransom, S. M. *et al.* Twenty-One Millisecond Pulsars in Terzan 5 Using the Green Bank Telescope. *Science* **307**, 892–896 (2005).

[20] Freire, P. C. C. *et al.* Eight New Millisecond Pulsars in NGC 6440 and NGC 6441. ApJ **675**, 670–682 (2008).

[21] Freire, P. C. C., Wolszczan, A., van den Berg, M. & Hessels, J. W. T. A Massive Neutron Star in the Globular Cluster M5. ApJ **679**, 1433–1442 (2008).

[22] Kurkela, A., Romatschke, P. & Vuorinen, A. Cold quark matter. Phys. Rev. D **81**, 105021 (2010).

[23] Lattimer, J. M. & Prakash, M. Ultimate Energy Density of Observable Cold Baryonic Matter. *Physical Review Letters* **94**, 111101 (2005).

[24] Cordes, J. M. & Lazio, T. J. W. NE2001.I. A New Model for the Galactic Distribution of Free Electrons and its Fluctuations. *ArXiv Astrophysics e-prints* (2002).

[25] Lattimer, J. M. & Prakash, M. Neutron Star Structure and the Equation of State. ApJ **550**, 426–442 (2001).

[26] Freire, P. *et al. in prep* (2010).

**Competing Interests** The authors declare that they have no competing financial interests.

**Correspondence** Correspondence and requests for materials should be addressed to P.B.D. (email: pdemores@nrao.edu).

| | |
|---|---|
| Ecliptic Longitude, $\lambda$ (deg) ............ | 245.78827556(5) |
| Ecliptic Latitude, $\beta$ (deg) ............. | -1.256744(2) |
| Proper Motion in $\lambda$ (mas yr$^{-1}$) ........ | 9.79(7) |
| Proper Motion in $\beta$ (mas yr$^{-1}$) ........ | -30(3) |
| Parallax (mas) ......................... | 0.5(6) |
| Pulsar Spin Period (ms) .............. | 3.1508076534271(6) |
| Period Derivative (s/s) ............... | 9.6216(9)$\times10^{-21}$ |
| Reference Epoch (MJD) ............... | 53600 |
| Dispersion Measure (pc cm$^{-3}$) ........ | 34.4865$^\dagger$ |
| Orbital Period (days) ................. | 8.6866194196(2) |
| Projected Semi-Major Axis (lt-s) ...... | 11.2911975(2) |
| 1$^{\text{st}}$ Laplace Parameter, $e\sin\omega$ ......... | 1.1(3)$\times10^{-7}$ |
| 2$^{\text{nd}}$ Laplace Parameter, $e\cos\omega$ ........ | -1.29(3)$\times10^{-6}$ |
| Companion Mass (M$_\odot$) ............... | 0.500(6) |
| Sine of Inclination Angle .............. | 0.999894(5) |
| Epoch of Ascending Node (MJD) ...... | 52331.1701098(3) |
| Span of Timing Data (MJD) .......... | 52469−55330 |
| Number of TOAs ..................... | 2,206 (454 / 1,752)$^\ddagger$ |
| RMS TOA Residual ($\mu$s) .............. | 1.1 |
| Right Ascension (J2000) .............. | 16$^{\text{h}}$ 14$^{\text{m}}$ 36$^{\text{s}}$.5051(5) |
| Declination (J2000) ................... | -22° 30′ 31″.081(7) |
| Orbital Eccentricity, $e$ ................. | 1.30(4)$\times10^{-6}$ |
| Inclination Angle (deg) ................ | 89.17(2) |
| Pulsar Mass (M$_\odot$) ..................... | 1.97(4) |
| DM-derived Distance (kpc) ........... | 1.2$^\S$ |
| Parallax Distance (kpc) ............... | >0.9 |
| Surface Magnetic Field (10$^8$ G) ........ | 1.8 |
| Characteristic Age (Gyr) .............. | 5.2 |
| Spin-down Luminosity (10$^{34}$ erg s$^{-1}$) .... | 1.2 |
| Average Flux Density at 1.4 GHz (mJy) | 1.2$^\dagger$ |
| Spectral Index, 1.1–1.9 GHz ............ | -1.9(1) |
| Rotation Measure (rad m$^{-2}$) .......... | -28.0(3) |

Table 1: Physical parameters for PSR J1614−2230: Timing model parameters (*top*); quantities derived from timing model parameter values (*middle*); radio spectral and interstellar medium properties (*bottom*). Timing values in parentheses represent 1-$\sigma$ uncertainty in the final digit, as determined by Markov chain Monte Carlo error analysis. †: These quantities vary stochastically on $\gtrsim$1-day timescales. Values presented here are the average for our GUPPI data set. ‡: Shown in parentheses are separate values for the long-term (first) and new (second) data sets described in the text. §: Calculated using the NE2001 pulsar distance model[24].